Event-Resolved Analysis of Neutron Detection by Organic Scintillators: Simulation and Analytical Solution

Sara A. Pozzi and Imre Pázsit *
Oak Ridge National Laboratory
P.O. Box 2008, MS 6010, Oak Ridge, TN37831-6010
e-mail: pozzisa@ornl.gov
(*)Department of Nuclear Engineering, Chalmers University of Technology
SE - 412 96 Göteborg, Sweden
e-mail: imre@nephy.chalmers.se

Accepted for Publication in the Proceedings of the INSTITUTE OF NUCLEAR MATERIALS MANAGEMENT (INMM) Annual Meeting July 16-20, 2006, Nashville, TN.

Event-Resolved Analysis of Neutron Detection by Organic Scintillators: Simulation and Analytical Solution

Sara A. Pozzi and Imre Pázsit *
Oak Ridge National Laboratory
P.O. Box 2008, MS 6010, Oak Ridge, TN37831-6010
e-mail: pozzisa@ornl.gov
(*)Department of Nuclear Engineering, Chalmers University of Technology
SE - 412 96 Göteborg, Sweden
e-mail: imre@nephy.chalmers.se

Abstract

Organic scintillators, in both liquid and plastic form, are commonly used in systems for the detection of nuclear materials in nonproliferation and homeland security applications. Neutron detection in this type of detector occurs by multiple scatterings on hydrogen (H) and carbon (C), the main constituents of the scintillator. The analysis of the statistics of neutron collisions is important to understand the mechanism of neutron detection, and to perform subsequent unfolding procedures aimed at determining the incident neutron spectrum.

We describe the Monte Carlo simulation of neutron interactions with the detector material for varying detector sizes and varying incident neutron energies. The simulations are performed using the code MCNP-PoliMi, which allows event-resolved predictions of the interactions of neutrons with the detector material. A subsequent post-processing of the simulation results allows us to determine the number of elastic collisions that the neutrons undergo with the nuclei of hydrogen and carbon atoms, together with the amount of energy that is deposited as a function of the number of collisions. The light output generated by proton recoils in hydrogen and carbon nuclei as a result of collisions with energetic neutrons from sources such as californium-252 (Cf-252) is also modeled, and the total detector efficiency is determined as a function of the incident neutron energy. When the neutron energy exceeds 4.4 MeV, inelastic scattering of neutrons from carbon nuclei can occur, generating subsequent gamma rays. This effect is taken into account and its contributions to the light output are discussed.

An analytical model is developed to describe the amplitude probability distribution of the light output generated in the scintillator for a monoenergetic flux of neutrons, taking into account the multiple collisions and the conversion of the deposited energy per collision to light pulses. The analytical model can be solved quantitatively by numerical quadrature. The possibility of including in the model neutron inelastic scattering and light generation by inelastic gamma rays is also investigated.

Introduction

For nuclear nonproliferation assays several measurement systems use liquid and plastic scintillators to detect neutrons and gamma rays from assemblies of fissile materials. [1]. Analysis of the neutron response functions of these detectors is essential to the development of unfolding techniques that can be used in neutron spectroscopy and neutron source identification methods [2]. The neutron response in these types of detectors is dominated by scattering on hydrogen, which is the mechanism that generates the most scintillation light. Neutron scattering on carbon, the other main constituent of the scintillator, produces significantly less light. However, scattering on carbon affects the detector response because each neutron can lose energy and, therefore, deposit less energy in subsequent interactions with hydrogen nuclei.

In this paper we present a detector response investigation that is based on an event-by-event statistical analysis of neutron histories in the detector. Quantities such as the number of collisions occurring in a scintillator are not measurable: what is measured is the combined effect of all collisions that contribute to a detector pulse. However, the *statistics* of the number of collisions is important when we consider neutron spectrum unfolding procedures. In fact, two effects, namely (i) nonlinearity in the light production from hydrogen scattering and (ii) small light output from carbon scattering, make the light output dependent not only on the *total* neutron energy deposited in the detector, but also on the *history* of the neutron energy deposition. We will determine the contribution of each of these effects in the remainder of this paper.

Monte Carlo Simulations

Our simulations were performed using the MCNP-PoliMi code [3]. The detector modeled consists of a cube having the dimensions 10 × 10 × 10 cm and a H:C composition in the ratio 0.548:0.452. This composition corresponds to that of the liquid scintillator BC-501 manufactured by Saint-Gobain.

Separate simulations were performed for each incident neutron energy interval, in the range 0 to 5 MeV in 0.1 MeV intervals, with neutron energies distributed uniformly in the 0.1 MeV intervals. The neutrons were incident perpendicularly on one of the faces of the detector cube, and uniformly distributed within the face.

The Monte Carlo output files record every neutron interaction that occurs in the detector volume, including interaction type, energy deposited, and collision nucleus (H or C). The energy deposited is then converted into light output, taking into account the identity of the collision nucleus (H or C). In the case of H, the relationship between energy deposited (T in MeV) and light output (L in MeVee) is

$$L = aT^2 + bT \equiv L(T) \qquad (1)$$

with a = 0.035 MeVee/MeV^2 and b = 0.141 MeVee/MeV for liquid scintillators. In the case of scattering on C, the light output is very small. F or this study we used the following relationship:

$$L\left(T\right) = cT \ , \qquad (2)$$

with c=0.02 MeVee/MeV.

Monte Carlo Results: Probability Distributions and Average Pulse Heights

Figure 1 (a) shows the relative probability that neutron histories will include *n* scatterings on hydrogen and *m* scatterings on carbon for incident neutrons having energy uniformly distributed in the interval 1 to 1.1 MeV, on a detector having dimensions 10 × 10 × 10 cm. The figure shows that the most probable event at this neutron energy and detector size is single scattering on hydrogen. Histories with only two scatterings on hydrogen (*n* = 2, *m* = 0) and only one scattering on carbon (*n* = 0 and *m* = 1) are approximately equally probable. Slightly less probable are histories with no interactions (*n* = 0 and *m* = 0) and histories with one scattering on carbon and one on hydrogen (*n* = 1 and *m* = 1).

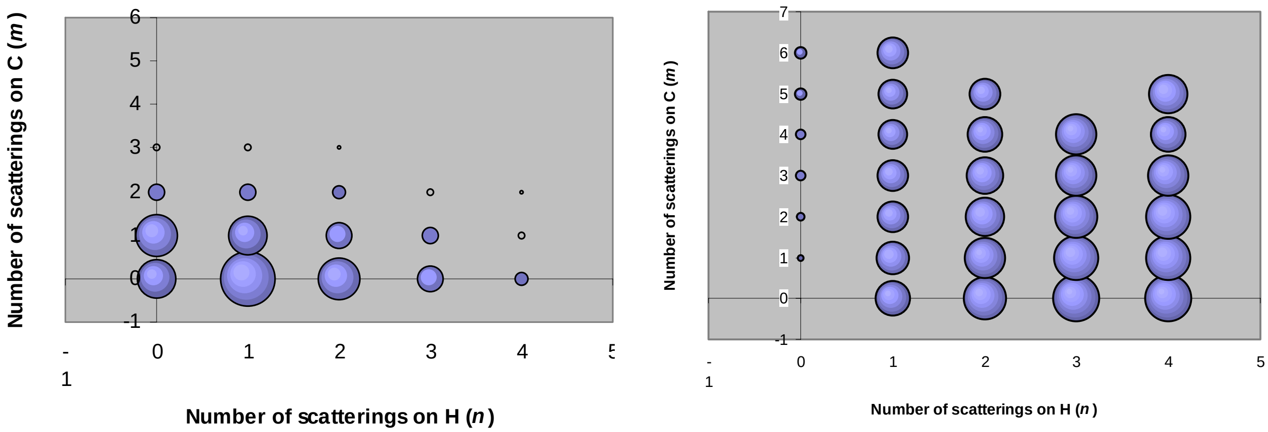

(a) (b)

Fig. 1 (a) Relative probability of neutron histories as a function of the number of scatterings on hydrogen (*n*) and on carbon (*m*) (1 to 1.1 MeV incident neutrons). (b) Average pulse heights as a function of the number of scatterings on hydrogen (*n*) and on carbon (*m*) (1- to 1.1-MeV incident neutrons).

Figure 1 (b) shows the average pulse height generated by neutron histories with *n* scatterings on hydrogen and *m* scatterings on carbon. In the figure, the radius of the sphere is proportional to an average pulse height for *n*, *m* scatterings on hydrogen and carbon, respectively. As expected, the histories having only scatterings on carbon do not generate much light in the detector (*n* = 0).

Single scatterings on hydrogen (*n* = 1, *m* = 0) generate less light than multiple scatterings on hydrogen (*n* = 2 to 4, *m* = 0).

Monte Carlo Results: Pulse Height Distributions

The Monte Carlo analysis allows us to calculate not only the average pulse height generated in the detector as a function of the *n* and *m* scatterings on hydrogen and carbon, but also the entire pulse height distribution. One such distribution is shown in Fig. 2 for 1-MeV incident neutrons. Figure 2 (a) shows the total pulse height distribution, and Fig. 2 (b) shows the contributions to the total distribution from histories comprising *n* and *m* scatterings on hydrogen and carbon, respectively, with *n* = 1, 2, and 3 and *m* = 0 and 1. Fig. 2 (b) shows that multiple scatterings on hydrogen contribute to increasing the detector response at higher pulse heights, whereas scatterings on carbon contribute to an increase in the detector response at lower pulse heights. The distribution labeled “Others” represents the cumulative contribution of all other combinations of *n* and *m* scatterings.

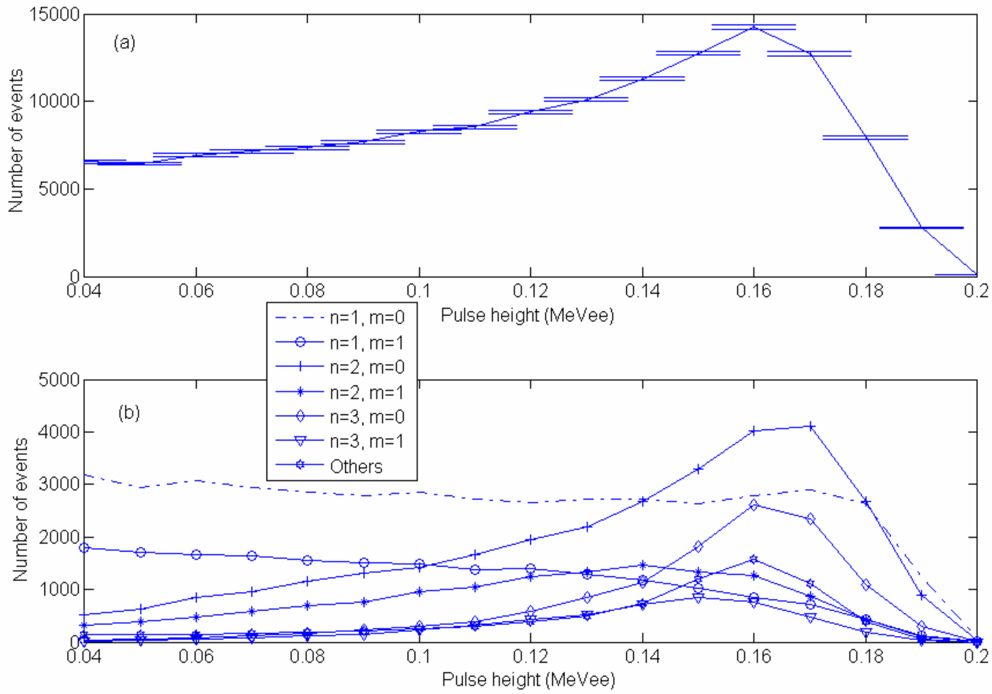

Fig. 2 Pulse height distributions for 1-MeV incident neutrons. (a) Total pulse height distribution is shown with error bars that represent statistical error. (b) Total is subdivided according to the total number of scatterings on hydrogen (*n* = 1, 2, and 3) and carbon (*m* = 0 and 1) in the neutron history. Error bars are not shown for clarity.

Detector Size

Figure 3 shows the pulse height distribution for 1MeV incident neutrons generated in two different detector sizes: a 10 × 10 × 10 cm detector (as in Fig. 2) and a 20 × 20 × 20 cm detector. In the larger detector, the pulse height distribution peaks at high pulse heights because of the increased probability of multiple scatterings of neutrons in collisions with hydrogen nuclei..

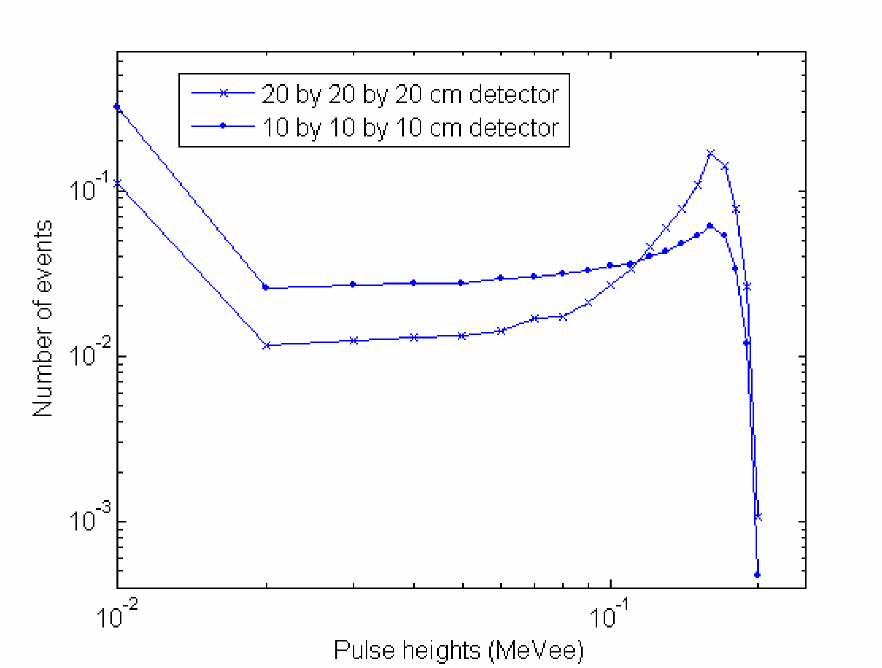

Fig. 3 Pulse height distributions for 1-MeV incident neutrons and two detector sizes.

Continuous Spectrum: Cf-252

When we consider a continuous neutron energy spectrum from Cf-252, the resulting pulse height distribution will be the sum of many distributions, such as those shown in Fig. 4. As a result, the cumulative distribution will typically include a broad continuum that extends up to the maximum light output generated by the neutrons having the highest energy, and an accumulation of many pulses at low pulse heights. In an experiment, the detector threshold setting in the data acquisition system will serve to cut the contributions at the low pulse heights.

Figure 4 (a) shows the pulse height distribution for Cf-252 neutrons impinging on a liquid scintillator. Note that the scale in the figure is now log-log. Figure 4 (b) shows the contributions to the total distribution from histories comprising n and m scatterings on hydrogen and carbon, respectively, with $n = 0$ to 3 and $m = 0$ to 3. Note that the histories comprising only scatterings on carbon ($n = 0$) contribute mainly to the low pulse heights.

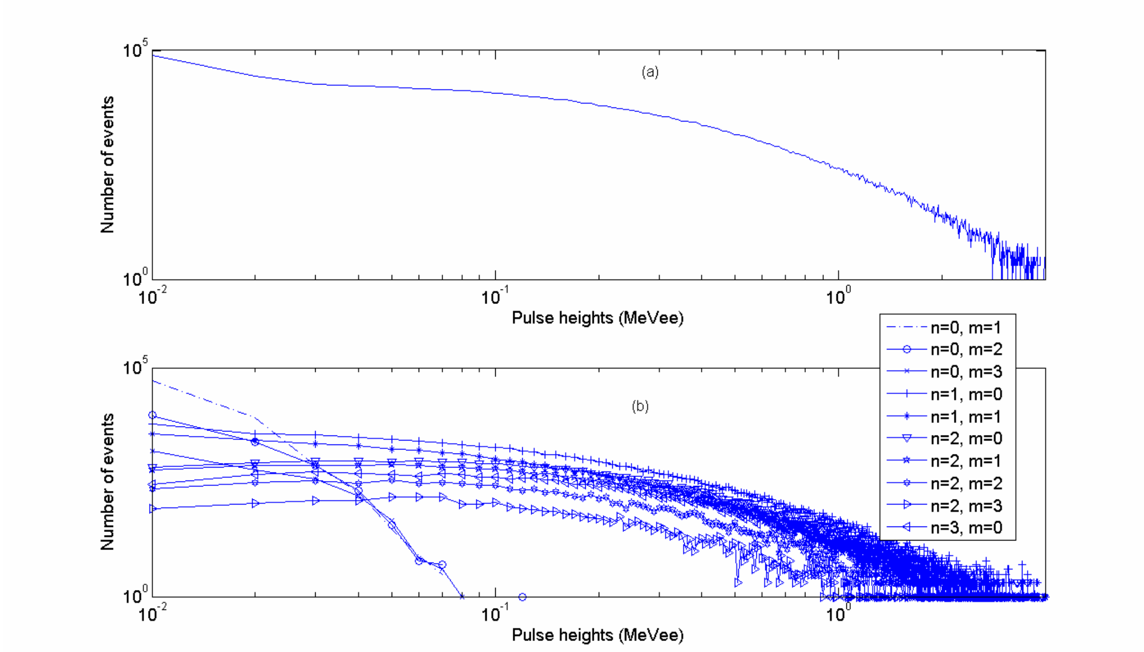

Fig. 4 Pulse height distributions for Cf-252 neutrons. (a) Total pulse height distribution. (b) The total is subdivided according to the total number of scatterings on hydrogen (*n* = 0, 1, 2, and 3) and carbon (*m* = 0, 1, 2, and 3) in the neutron history. Error bars are not shown for clarity.

Figure 5 shows a comparison between experimental data [4] and simulated data. The experimental data were acquired with the detector threshold set at approximately 0.12 MeVee. As can be seen, there is very good agreement between the simulated and measured data: the average relative error was approximately 6% in the pulse height range 0.12 to 1.12 MeVee. The comparison shown in Fig. 5 serves as a validation for the Monte Carlo approach.

In addition to providing an estimate of the total pulse height distribution, Monte Carlo can be used to simulate the individual components, such as those shown in Fig. 4 (b). This ability is essential in the analysis of the response of existing detectors and in the development of new detector types.

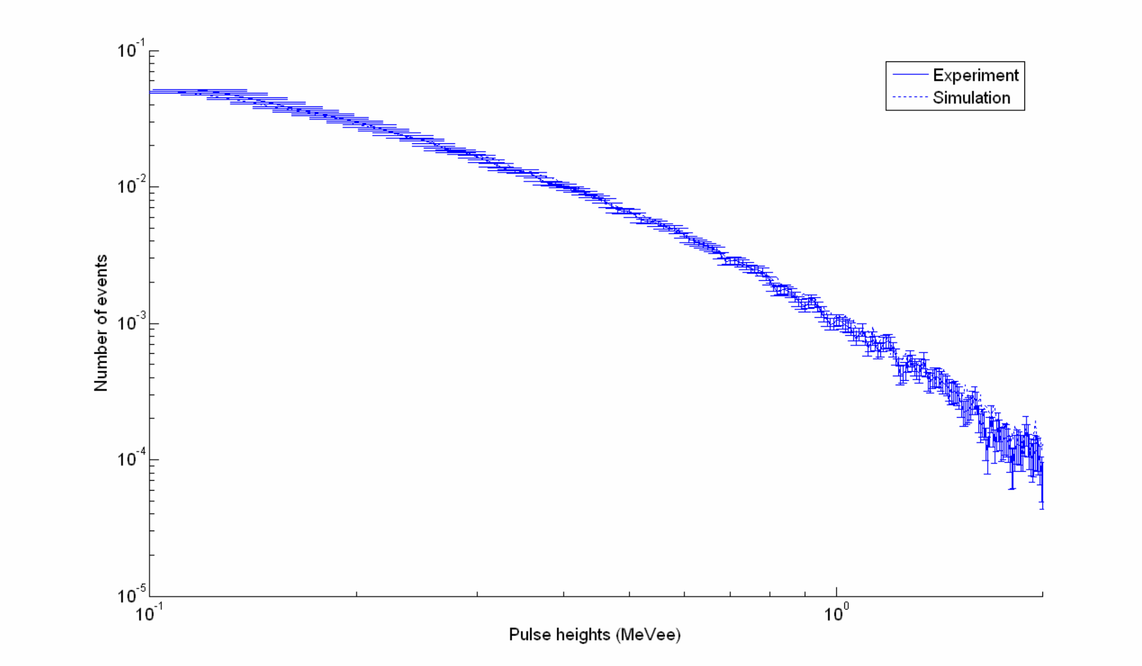

Fig. 5 Pulse height distributions for Cf-252 neutrons. Experimental data shown with error bars, simulation shown with dotted line.

Analytical Approach and Discussion

The distribution of the energy transferred (T) by a neutron having incoming energy E_0, in a single collision with hydrogen is equal to

$$p(T, E_0)dT = \frac{dT}{E_0}, \tag{3}$$

where, as expected, $p(T, E_0)$ is independent of the amount of energy transferred, T. It follows that the distribution of light generated in the detector by a neutron having incident energy E_0 is

$$f_1(L, E_0) = \frac{1}{E_0\sqrt{b^2 + 4aL}}, \tag{4}$$

with L lying between 0 and $L_{max} = aE_0{}^2 + bE_0$. For a given light intensity L in (4), the transferred energy is given as

$$T(L) = \frac{\sqrt{b^2 + 4aL} - b}{2a} \tag{5}$$

That is, f_1 is relatively flat since $a<<b$, and it decreases slowly for increasing light intensities, as shown in Figure 6 (b).

From here the distribution of the light generated by neutrons colliding more than one time with hydrogen can be calculated by convolution-type integrals. For the distribution after two collisions, $f_2(L,E_0)$, one has:

$$f_2(L,E_0)=\int_0^L f_1(L-l,E_0-T(l))\,f_1(l,E_0)dl = \\ =\frac{1}{E_0}\int_0^L \frac{1}{E_0-T(l)\sqrt{b^2+4a(L-l)}}\frac{1}{\sqrt{b^2+4al}}dl \quad , \qquad (6)$$

where $T(l)$ is given by Eq. (5).

The integral in (6) can be calculated numerically and is shown in Figure 6(b). As can be seen, there is general agreement in the shape of f_1 and f_2 between the Monte Carlo simulations (Fig. 6 (a)) and the analytical solution (Fig. 6 (b)).

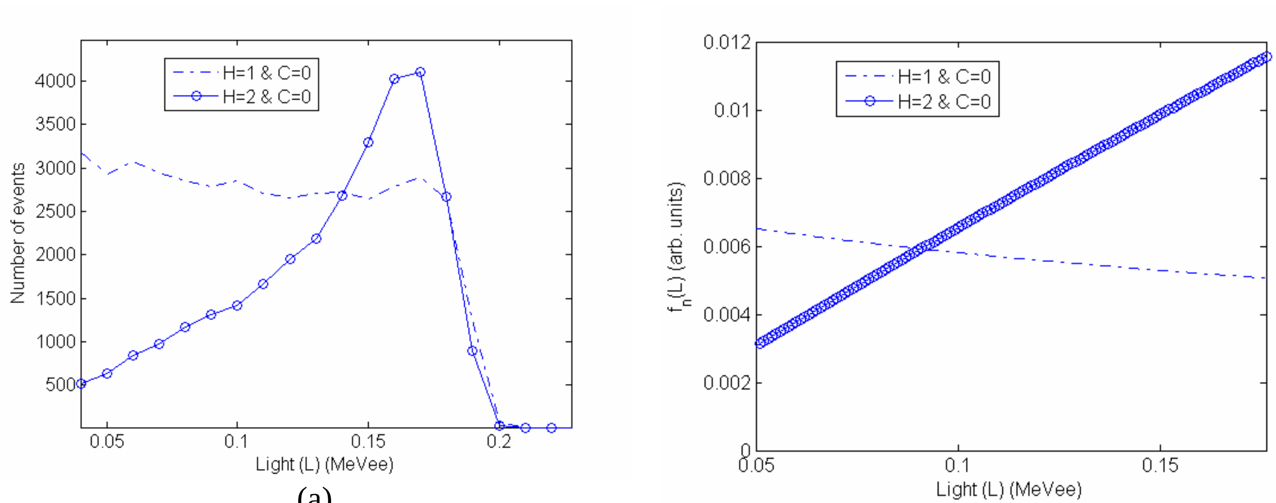

(a)

(b)

Fig. 6 (a) Monte Carlo simulation of light output for 1-MeV incident neutrons in the case of one scattering on hydrogen and two scatterings on hydrogen. (b) Analytical solution of the light output for the case of one scattering on hydrogen and two scatterings on hydrogen (1-MeV incident neutrons).

References

1. J. T. Mihalczo, J. A. Mullens, J. K. Mattingly, T. E. Valentine, "Physical Description of Nuclear Materials Identification System (NMIS) Signatures," *Nuclear Instruments and Methods in Physics Research A*, **450**/2-3, pp. 531-555, 2000.
2. S. Avdic, S. A. Pozzi, and V. Protopopescu, “Detector Response Unfolding Using Artificial Neural Networks”, accepted for publication in *Nuclear Instruments and Methods in Physics Research Section A.*
3. S. A. Pozzi, E. Padovani, and M. Marseguerra, “MCNP-PoliMi: A Monte Carlo Code for Correlation Measurements,” *Nuclear Instruments and Methods in Physics Research A*, **513**/3, pp. 550, 2003.
4. S. A. Pozzi and S. Avdic, “Neutron and Gamma Ray Pulse Shape Data Acquisition from a Cf-252 Source,” ORNL TM 2006/62.